Nuclear dynamics at the balance energy

Aman D. Sood and Rajeev K. Puri
Physics Department, Panjab University, Chandigarh 160 014, India
(Received 6 September 2003; published 30 September 2004)

We study the mass dependence of various quantities (like the average and maximum density, collision rate, participant-spectator matter, and temperature, as well as time zones for higher density) by simulating different reactions at the energy of vanishing flow. This study is carried out within the framework of the quantum molecular dynamics model. Our findings clearly indicate the existence of a power law in all the above quantities calculated at the balance energy. A significant mass dependence exists for the temperature reached in the central sphere. All other quantities at the balance energy are either rather insensitive or depend weakly on the system size. The time zone for the higher density as well as the time of maximal density and collision rate follow a power law inverse to the energy of vanishing flow. The participant matter at the balance energy shows a remarkable lack of mass dependence that makes it a good candidate for studying the balance energy.

DOI: 10.1103/PhysRevC.70.034611 PACS number(s): 25.70.Pq

I. INTRODUCTION

It is now well established that interactions at low incident energies are dominated by the attractive part of the nuclear mean field causing the emission of particles in the backward angles. These interactions, however, become repulsive at higher incident energies, pushing the particles into the forward (positive) angles. While going from low incident energies to higher incident energies, there happens a particular energy at which the net in-plane transverse flow disappears [1]. This energy (termed the "balance energy") E_{bal} has been reported to be of significance toward the understanding of nuclear interactions and related dynamics [2–24].

Recently, E_{bal} was measured for ^{197}Au+^{197}Au collisions [4,5], extending the mass range of E_{bal} between 24 and 394 units. In addition to ^{197}Au+^{197}Au collisions, E_{bal} has also been measured in ^{12}C+^{12}C [7], ^{20}Ne+^{27}Al [7], ^{36}Ar+^{27}Al [9,12], ^{40}Ar+^{27}Al [8], ^{40}Ar+^{45}Sc [5,7,13], ^{40}Ar+^{51}V [10], ^{64}Zn+^{27}Al [11], ^{40}Ar+^{58}Ni [6], ^{64}Zn+^{48}Ti [12], ^{58}Ni+^{58}Ni [5,6,13], ^{58}Fe+^{58}Fe [13], ^{64}Zn+^{58}Ni [12], ^{86}Kr+^{93}Nb [5,7], ^{93}Nb+^{93}Nb [3], ^{129}Xe+^{118}Sn [6], and ^{139}La+^{139}La [3] collisions. One notices that most of the above reactions are symmetric and central in nature. Some attempts are also reported in the literature that deal with the impact parameter dependence of the balance energy E_{bal} [5,6,8,11,13,17,20,21].

Interestingly enough, most of the theoretical attempts at the disappearance of flow are within the Boltzmann-Uehling-Uhlenbeck model [1,3–5,7,8,11,13,15–18]. Some attempts, however, have also been made within the framework of the quantum molecular dynamics (QMD) model [13,19–24]. Note that, among all these attempts, only a few deal with the mass dependence of the disappearance of flow [4,5,7,18,22–24]. There, a power law behavior ($\propto A^{\tau}$) in E_{bal} has been reported. For the first time, a complete study of the mass dependence of balance energy was presented by us where as many as 16 systems with masses between 47 and 476 were analyzed [22–24]. Excellent agreement between experimental measurements and our theoretical calculations allowed us to predict the balance energy in ^{238}U+^{238}U collisions around 37–39 MeV/nucleon [22]. Note that none of the above studies were extended to other heavy-ion phenomena at the balance energy. References [11,15,18,20,21] give some information about the nature of the other variables at the balance energy.

Our present aim is at least twofold: (i) To present a complete analysis of the nuclear dynamics at the balance energy by analyzing more than 14 (nearly symmetric) reactions as reported in Refs. [23,24] and (ii) to look for the other observables and nonobservables that can be used as alternatives to study the energy of vanishing flow. It has been suggested that the attractive and repulsive forces do counterbalance each other at the balance energy; it is, therefore, highly desirable to investigate the effect of such counterbalancing in different (non)observables.

This study is made within the framework of the quantum molecular dynamics model, which is described in detail in several previous studies [19–29].

Our results along with the discussion are presented in Sec. II. We summarize the results in Sec. III.

II. RESULTS AND DISCUSSION

As stated in Ref. [23], a hard equation of state along with an energy independent *NN* cross section of 40 mb strength yields a power law behavior proportional to A^{τ}. The power law (cA^{τ}) over the experimental points yields $\tau = -0.42 \pm 0.046$, whereas our theoretical calculations with a *NN* cross section of 40 mb strength gave $\tau = -0.42 \pm 0.082$ [23]. It is worth mentioning that this is the closest agreement obtained so far by any theoretical attempt. For the present mass dependent analysis, we simulated the reactions of ^{20}Ne+^{27}Al ($b/b_{max}=0.4$), ^{36}Ar+^{27}Al ($b=2.5$ fm), ^{40}Ar+^{27}Al ($b=1.6$ fm), ^{40}Ar+^{45}Sc ($b/b_{max}=0.4$), ^{40}Ar+^{51}V ($b/b_{max}=0.3$), ^{40}Ar+^{58}Ni ($b=0-3$ fm), ^{64}Zn+^{48}Ti ($b=2$ fm), ^{58}Ni+^{58}Ni ($b/b_{max}=0.28$), ^{64}Zn+^{58}Ni ($b=2$ fm), ^{86}Kr+^{93}Nb ($b/b_{max}=0.4$), ^{93}Nb+^{93}Nb, ($b/b_{max}=0.3$) ^{129}Xe+^{nat}Sn ($b=0-3$ fm), ^{139}La+^{139}La ($b/b_{max}=0.3$), and ^{197}Au+^{197}Au ($b=2.5$ fm) at

their corresponding theoretical balance energies,[1] which are, respectively, 119, 74, 67.3, 89.4, 67.8, 64.6, 59.3, 62.6, 56.6, 69.2, 57, 49, 51.6, and 43 MeV/nucleon. The choice of the impact parameters is guided by the experimental measurements. The reactions were followed until the nuclear in-plane transverse flow saturated. As noted above, the balance energy is smaller in heavier colliding nuclei, compared to the lighter ones. As a result, one would expect early saturation in the lighter colliding nuclei compared to the heavy ones. Although the transverse flow saturates much earlier in lighter nuclei, some variables keep changing; therefore, we follow all the reactions uniformly up to 1200 fm/c.

In the following, we shall first study the time evolution and then present the mass dependence of different quantities.

A. The time evolution

One of the motivations behind studying heavy-ion collisions is to extract information about the hot and dense nuclear matter. In our approach, matter density is calculated by [29]

$$\rho(\vec{r},t) = \sum_{i=1}^{A_T+A_P} \frac{1}{(2\pi L)^{3/2}} e^{\{-[\vec{r}-\vec{r}_i(t)]^2/2L\}}. \quad (1)$$

Here A_T and A_P stand, respectively, for the mass of the target and projectile. In actual calculations, we take a sphere of 2 fm radius around the center of mass and compute the density at each time step during the reaction using Eq. (1). Naturally, one can either extract an average density $\langle \rho^{avg} \rangle$ over the whole sphere or a maximal value of the density $\langle \rho^{max} \rangle$ reached anywhere in the sphere.

In Fig. 1(a), we display $\langle \rho^{avg} \rangle / \rho_0$ whereas Fig. 1(b) shows the $\langle \rho^{max} \rangle / \rho_0$ as a function of the reaction time. The displayed reactions are ^{20}Ne+^{27}Al (A=47), ^{40}Ar+^{45}Sc (A=85), ^{64}Zn+^{58}Ni (A=122), ^{93}Nb+^{93}Nb (A=186), ^{139}La+^{139}La (A=278), and ^{197}Au+^{197}Au (A=394), spreading over the whole mass range. It is evident that the maximal ρ^{avg} for lighter systems is slightly higher than for the heavy ones. A similar trend can also be seen for the evolution of ρ^{max}. Further, the maximal and average densities are comparable for the medium and heavy systems, indicating that the dense matter is formed widely and uniformly in the central region of 2 fm radius. On the other hand, a substantial difference in the two densities for the lighter colliding nuclei indicates the nonhomogenous nature of the dense matter. Due to the high incident energy, the ^{20}Ne+^{27}Al reaction finishes much earlier compared to ^{197}Au+^{197}Au which is simulated at a relatively lower incident energy. Similarly, the peaks in (the maximum $\langle \rho^{max} \rangle$ and average $\langle \rho^{avg} \rangle$) densities are also delayed in heavier nuclei compared to the lighter ones. The wider density zones in heavier colliding nuclei over a long time span indicates the ongoing interactions among the nucleons which is in agreement with [29].

[1]The theoretical balance energy was calculated by extrapolating the flow at two different energies with a step of ±10 MeV/nucleon [23].

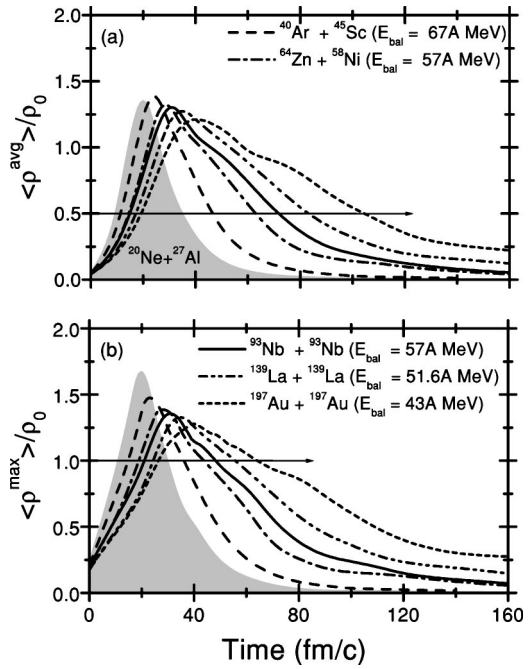

FIG. 1. The evolution of (a) average density $\langle \rho^{avg} \rangle$ and (b) the maximum density $\langle \rho^{max} \rangle$ reached in a central sphere of radius 2 fm as a function of time. Here reactions of ^{20}Ne+^{27}Al, ^{40}Ar+^{45}Sc, ^{64}Zn+^{58}Ni, ^{93}Nb+^{93}Nb, ^{139}La+^{139}La, and ^{197}Au+^{197}Au are simulated at their corresponding theoretical balance energies (for details, see the text). The shaded area represents the reaction of ^{20}Ne +^{27}Al.

Another quantity linked directly with the density is the collision rate. In Fig. 2, we display the net collision rate as a function of the reaction time. Due to the larger interaction volume in heavy nuclei, the interactions among nucleons continue for a longer time, which is also evident from the density profile (see Fig. 1). Further, a finite extended density zone in heavier nuclei leads to more *NN* collisions.

Since the balance energy represents a counterbalancing between the attractive and repulsive forces, this fact should also be reflected in quantities like the spectator and participant matter. In the present study, we define the participant

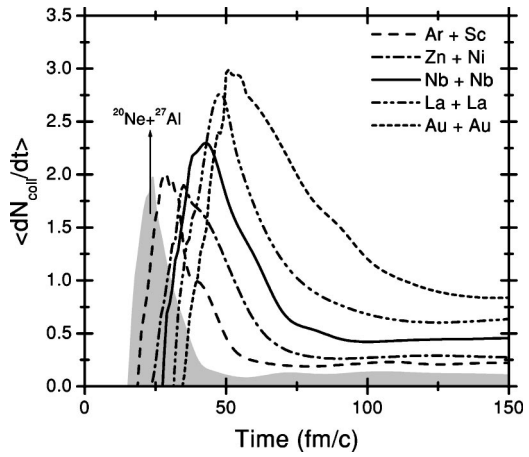

FIG. 2. Same as Fig. 1(a), but the rate of allowed collisions dN_{coll}/dt versus reaction time.

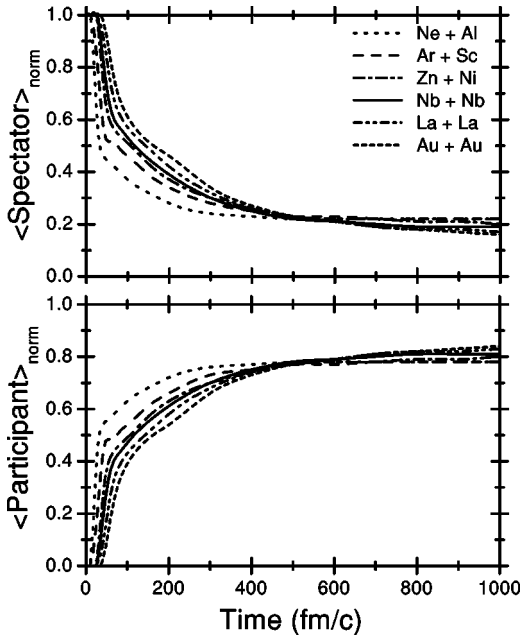

FIG. 3. Same as Fig. 1, but the time evolution of the normalized spectator matter (upper part) and participant matter (lower part) defined in terms of nucleon-nucleon collisions.

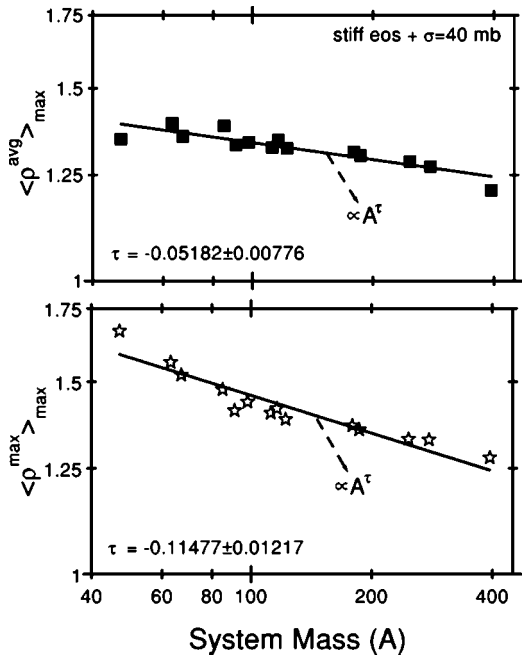

FIG. 4. The maximal value of the average density $\langle\rho^{avg}\rangle_{max}$ (upper part) and maximum density $\langle\rho^{max}\rangle_{max}$ (lower part) as a function of the composite mass of the system. The solid lines are the fits to the calculated results using cA^{τ} obtained with χ^2 minimization.

matter in two different ways. (i) All nucleons having experienced at least one collision are counted as *participant matter*. The remaining matter is labeled as *spectator matter*. The nucleons with more than one collision are labeled as *super-participant matter*. These definitions give us a possibility of analyzing the reaction in terms of the participant-spectator fireball model. These definitions, however, are more of theoretical interest since the matter defined in these zones cannot be measured. (ii) Alternatively, we define the participant and spectator matter in terms of the rapidity distribution:

$$Y(i) = \frac{1}{2}\ln\frac{\mathbf{E}(i) + \mathbf{p}_z(i)}{\mathbf{E}(i) - \mathbf{p}_z(i)}, \tag{2}$$

where $\mathbf{E}(i)$ and $\mathbf{p}_z(i)$ are, respectively, the total energy and longitudinal momentum of the ith particle. We shall rather use a reduced rapidity $Y_{red}(i) = Y(i)/Y_{beam}$. Here different cuts in the rapidity distributions can be imposed to define the different participant matter. This method is used often in the literature for experimental analysis [30]. We shall define normalized participant matter by imposing three different cuts: all nucleons with (i) $-1.0 \leqslant Y_{red}(i) \leqslant +1.0$ (labeled as "A"), (ii) $-0.75 \leqslant Y_{red}(i) \leqslant +0.75$ (marked as "B"), and (iii) $-0.5 \leqslant Y_{red}(i) \leqslant +0.5$ (marked as "C"). These three different definitions give us a possibility of examining the participant matter at the balance energy that can be verified experimentally.

In Fig. 3, we display the normalized spectator matter (upper part) and participant matter (lower part) as a function of the reaction time. Here participant matter is defined using the nucleonic concept. The results are, however, similar for both the definitions. At the start of the reaction, all nucleons constitute spectator matter. Therefore, no participant matter exists at $t = 0$ fm/c. Since the ^{20}Ne+^{27}Al reaction happens at a relative higher energy (=119 MeV/nucleon), the transition from the spectator to participant matter is swift and sudden. On the other hand, due to the low bombarding energy in heavier colliding nuclei, the transition from the spectator to participant matter is slow and gradual. Interestingly, at the end, all the reactions (that happen between incident energies 43 and 119 MeV/nucleon) lead to (nearly) the same participant matter, indicating the universality in balancing the attractive and repulsive forces. This will be discussed in detail in the following paragraphs.

From the above facts, it is clear that the heavier colliding nuclei (at E_{bal}) lead to an extended density profile. It will be interesting to see whether these findings depend on the masses of the colliding nuclei or not. This will be discussed in the following paragraphs.

B. The mass dependence

In Fig. 4, we display the maximal value of $\langle\rho^{avg}\rangle$ and $\langle\rho^{max}\rangle$ versus the composite mass of the system. Note that most of the reactions considered here are symmetric in nature, i.e., $\eta|(A_t - A_P)/(A_T + A_P)| < 0.2$. Interestingly, the maximal value (of $\langle\rho^{avg}\rangle$ and $\langle\rho^{max}\rangle$) follows a power law proportional to A^{τ} with τ being -0.05 ± 0.008 for the average density $\langle\rho^{avg}\rangle$ and -0.11 ± 0.012 for the maximum density $\langle\rho^{max}\rangle$.[2] In other words, a slight decrease in the density occurs with increasing size of the system. This decrease is much smaller compared to E_{bal} ($\tau_{expt} = -0.42 \pm 0.046$ and $\tau_{th} = -0.42 \pm 0.082$). Had these reactions been simulated at a fixed incident energy, the trend would have been totally dif-

[2]A small deviation can be seen in the cases when $\eta \neq 0$.

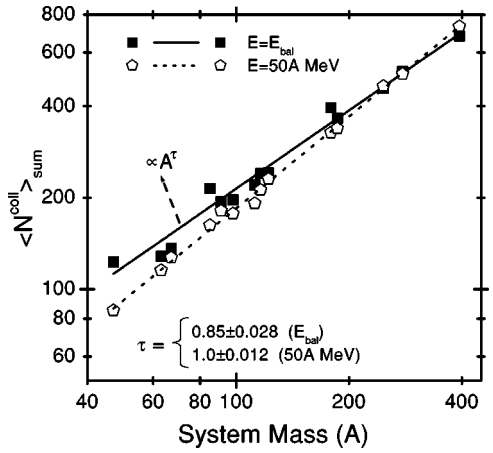

FIG. 5. The total number of the allowed collisions (obtained at the final stage) versus composite mass of the system. The solid squares and open pentagons are the results obtained at E_{bal} and 50 MeV/nucleon, respectively. The solid and dashed lines are the fits obtained with the procedure explained in Fig. 4.

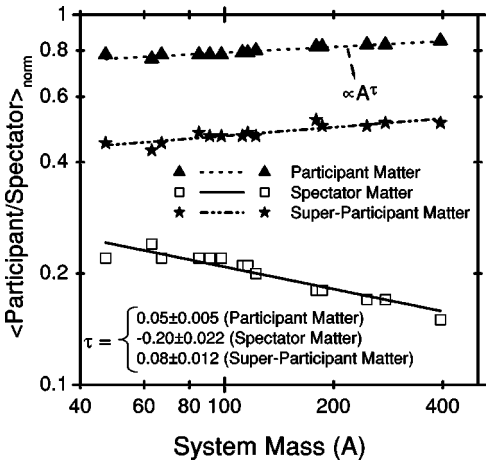

FIG. 6. Same as Fig. 5, but for the final saturated participant, spectator, and superparticipant matter defined in terms of nucleon-nucleon collisions.

ferent [29]. Since lighter nuclei cannot be compressed easily, their maximal density at a fixed incident energy will be less compared to the heavy nuclei.

The mass dependence of the (allowed) *NN* collisions is depicted in Fig. 5. The results are displayed at 1200 fm/c where matter is very diluted and well separated. Here one sees a (nearly) linear enhancement in the *NN* collisions with the size of the interacting system. This enhancement can be parametrized with a power law proportional to A^{τ}; $\tau = 0.85 \pm 0.028$. Naturally, at a fixed energy, the *NN* collisions should scale as A. To test this, we also display in Fig. 5, the *NN* collisions at 50 MeV/nucleon. This rate can be parametrized well by a power law with $\tau = 1.0 \pm 0.012$, indicating the linear relationship between the mass of the system and *NN* collisions at a fixed incident energy.

A dynamical quantity that can serve as an indicator of the role of repulsive and attractive forces is the participant and spectator matter. Naturally, the possibility of a collision (and hence of spectator and participant matter) will depend upon the mean free path of the nucleons. In Fig. 6, we display the spectator, participant, and superparticipant matter (obtained at 1200 fm/c and defined in terms of nucleon-nucleon collisions) as functions of the total mass of the system. Interestingly, we see a nearly mass independent behavior of the participant matter ($\tau = 0.05 \pm 0.005$). Similar behavior also occurs in the case of spectator matter $\tau = -0.20 \pm 0.022$. The superparticipant matter shows ($\tau = 0.08 \pm 0.012$). A slight deviation can be seen in the ^{20}Ne+^{27}Al reaction. Some small fluctuations can also be due to the variation in the impact parameter, which is not fixed in the present study. It should also be kept in mind that an asymmetric colliding pair does not follow the power law of a symmetric colliding pair in the first place. The choice of the impact parameter is guided by the experimental measurements. As noted in Ref. [21], the variation in the impact parameter can also have a drastic influence on the participant and spectator matter.

In Fig. 7, we again display the participant matter, defined in terms of the different rapidity cuts. Interestingly, we see a remarkable mass independent nature of the participant matter. The participant matter consisting of nucleons with $-1.0 \leqslant Y_{red}(i) \leqslant +1.0$ follows a power law with $\tau = -0.007 \pm 0.009$, whereas participant matter with nucleons $-0.75 \leqslant Y_{red}(i) \leqslant +0.75$ has $\tau = 0.015 \pm 0.019$. If one defines the participant matter in terms of nucleons with $-0.5 \leqslant Y_{red}(i) \leqslant +0.5$, $\tau = 0.04 \pm 0.031$. In other words, whether one defines the participant matter in terms of nucleon-nucleon collisions or in terms of rapidity distribution cuts, both yield the same results. The visible fluctuations in this figure might be due to several causes. (i) By imposing cuts in the rapidity distributions, the number of nucleons falling in a particular zone decreases, which leads to fluctuations. (ii) As stated above, the impact parameter (which is guided by the experimental choice) is not uniform in the present reactions. This impact parameter variation can also lead to some fluctuations. (iii) The asymmetry of the colliding nuclei is also not fixed, which further adds to the fluctuations. Similar scatterings around the mean values are also visible in the plots of balance energy versus mass of the system [4,7,24]. To strengthen our argument, we simulated five symmetric reac-

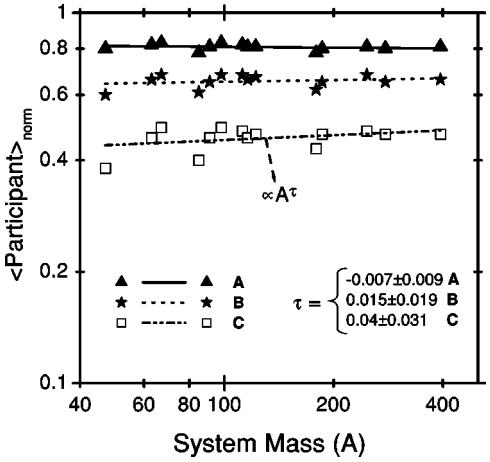

FIG. 7. Same as Fig. 6, but using different rapidity distribution cuts. For the details of A, B and C, see the text.

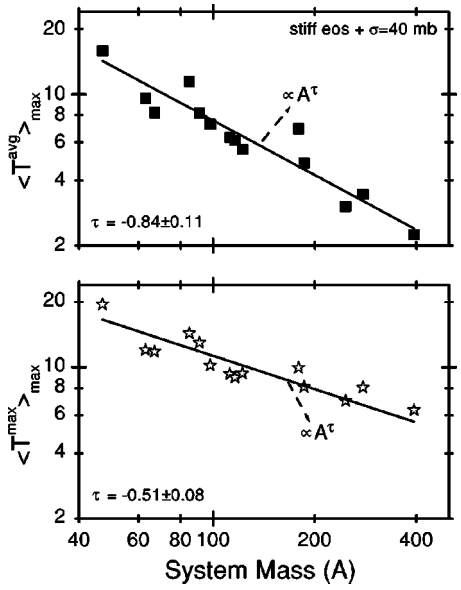

FIG. 8. Same as Fig. 5, but for the maximal value of the average temperature (upper part) and maximum temperature (lower part).

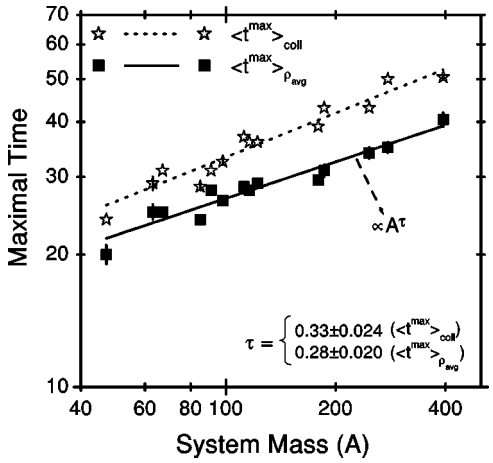

FIG. 9. Same as Fig. 5, but for the time of maximal value of collision rate (open stars) and average density (solid squares). The solid and dashed lines represent the χ^2 fits with power law cA^{τ}.

tions, ^{20}Ne+^{20}Ne, ^{40}Ca+^{40}Ca, ^{58}Ni+^{58}Ni, ^{93}Nb+^{93}Nb, and ^{197}Au+^{197}Au at a reduced impact parameter ($b/b_{max}=0.40$) and at several incident energies. The balance energy and participant matter were then deduced in each case using different rapidity cuts. Remarkably, we found (not shown here) that all the points fall on a power law curve with τ very close to zero. This analysis supports our above argument that the scattering around the mean value is due to the impact parameter and asymmetry variation in the above mentioned reactions.

The above mass independent behavior can be explained in terms of the density profile (Fig. 4). There one concluded that the lighter nuclei led to higher densities. In other words, the mean free path will be smaller in lighter nuclei, which results in more *NN* collisions. One should keep in mind that the mass independent nature of the participant matter is not a trivial observation. For a fixed system mass, the participant matter depends linearly on the incident energy. In the present case, although the mass of the system increases, their corresponding incident energy decreases, resulting in the net mass independent nature. This also indicates that the repulsive and attractive forces at E_{bal} counterbalance each other in such a manner that the net participant matter remains the same in all cases. One may also say that, since the contribution of the mean field toward transverse flow is nearly mass independent [23,31], one needs the same amount of participant matter to counterbalance the attractive forces. In other words, the participant matter can act as a barometer to study the balance energy in heavy-ion collisions.

The associated quantity linked with the dense matter is the temperature. In principle, a true temperature can be defined only for thermalized and equilibrated matter. Since in heavy-ion collisions the matter is nonequilibrated, one cannot talk of "temperature." One can, however, look in terms of the local environment only. In our present case, we follow the description of the temperature given in Refs. [29,32]. Several authors have given different descriptions of the local or global temperatures [33–36]. Some authors define temperature in terms of the fireball model [33], whereas others extracted the temperature from the measured pion yields and got a reasonable system temperature [34]. In Ref. [35], the thermalization is directly connected with the nondiagonal elements of the stress tensor. The "transverse" temperature has even been defined in terms of $\langle P_I^2/2m\rangle$; P_I^2 is the average transverse momentum squared [34]. In the present case, extraction of the temperature T is based on the local density approximation, i.e., one deduces the temperature in a volume element surrounding the position of each particle at a given time step [29,32]. Here, we postulate that each local volume element of nuclear matter in coordinate space and time has some "temperature" defined by the diffused edge of the deformed Fermi distribution consisting of two colliding Fermi spheres, which is typical for a nonequilibrium momentum distribution in heavy-ion collisions.

In this formalism (dubbed the hot Thomas-Fermi approach [29]), one determines extensive quantities like the density and kinetic energy as well as the entropy with the help of momentum distributions at a given temperature. For more details, the reader is referred to Refs. [29,32]. Using this formalism, we also extracted the average and maximum temperature within a central sphere of 2 fm radius as described in the case of density.

In Fig. 8, we plot the maximal values of $\langle T^{avg}\rangle$ and $\langle T^{max}\rangle$ as functions of the composite mass of the system. Some fluctuations might be due to the choice of the impact parameter as well as the incident energy [29,32,34,37,38]. As stated above, the impact parameter choice is guided by the experimental constraints. Further, E_{bal} was extracted using a straight line interpolation; therefore, both these factors may add to the present fluctuations. One sees that both these quantities can be parametrized in terms of a power law function proportional to A^{τ}; to the power factor τ is quite large (being equal to -0.84 ± 0.11 and -0.51 ± 0.08, respectively, for the average and maximal temperatures). This sharp mass dependence in the temperature is rather in contradiction to the mild mass dependence obtained in all other quantities. This is not astonishing since the temperature depends, cru-

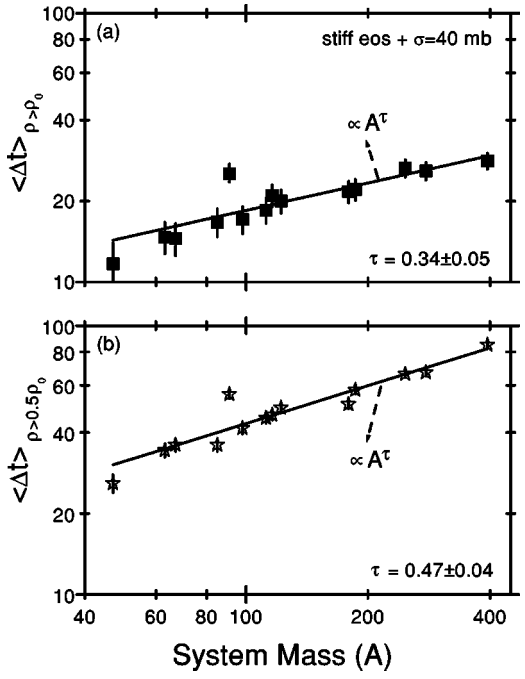

FIG. 10. Same as Fig. 8, but for the time zone for $\rho \geqslant \rho_0$ (upper part) and for $\rho \geqslant \rho_0/2$ (lower part) as a function of composite mass of the system.

cially, on the kinetic energy (or the excitation energy) of the system [29,32,37,38]. It was shown in Refs. [37,38] that for a given colliding geometry the maximal value of temperature does not depend upon the size of the interacting source. Rather it depends only on the bombarding energy. As noted in Ref. [37], the extraction of the temperature using the hot Thomas-Fermi formalism was in good agreement with the values extracted from the pion yields. Therefore, our prediction can be tested using measured pion yields.

In Fig. 9, we display the time of the maximal collision rate and average density. We see a power law behavior in both quantities. The low balance energies in heavy nuclei delay the maximal compression. Interestingly, the power factor τ is close to $1/3$ in both cases. E_{bal} was shown to have power factor $\tau \approx -0.4$. In other words, the time of maximal collision rate and density vary approximately as the inverse of E_{bal}.

Apart from the maximal quantities, another interesting quantity is the dense zone at the balance energy. This is depicted in Fig. 10 where we display the time interval for which $\rho \geqslant \rho_0$ (upper part) and $\rho \geqslant \rho_0/2$. Again both quantities follow a power law behavior. Interestingly, the time intervals for the high density have a power law dependence with $\tau = 0.34 \pm 0.054$ and $\tau = 0.47 \pm 0.04$, respectively, for $\rho \geqslant \rho_0$ and $\rho \geqslant \rho_0/2$, which are again very close to the inverse of the mass dependence of E_{bal}. This also points toward the fact that the formation and identification of the fragments is delayed in heavier nuclei compared to the lighter nuclei. This conclusion is in agreement with earlier calculations [28,38].

We also studied the influence of the variation in the surface properties of nuclei on the energy of vanishing flow and also on other variables reported in this paper. This was done by simulating the above mentioned reactions using two Gaussian widths: (i) $L = 4.33$ fm^2 as in the present case and (ii) a wider Gaussian with $L = 8.66$ fm^2. Although visible effects were noted in the energy of vanishing flow, the power factors τ for the present quantities remain nearly the same, suggesting that the different Gaussian widths do not affect our conclusions above.

III. SUMMARY

Using the QMD model, we presented the mass dependence of various quantities (such as the average and maximum central density, temperature, collision dynamics, and participant and spectator matter, as well as the time zone for hot and dense nuclear matter) at the energy of vanishing flow (E_{bal}). This study was conducted using a hard equation of state along with a *NN* cross section of 40 mb strength. This combination is reported to explain the experimentally extracted balance energy for a large number of cases [23]. Our calculations present several interesting facts.

The reaction saturation time is smaller for the lighter nuclei compared to the heavy ones. The maximal values of the density, temperature, and collision rate are also shifted accordingly. In all the cases (i.e., in the average and maximum central density, temperature, participant and spectator matter, etc.), a power law dependence can be seen. The only quantity where the power factor τ is significant (with $\tau \geqslant |0.2|$) is the temperature reached in the central zone. Other quantities are nearly mass independent. The mass independent nature of the participant matter makes it a good alternative indicator for determining the balance energy that can be measured experimentally, and our predictions can be verified.

ACKNOWLEDGMENT

This work is supported by Grant No. SP/S2/K-21/96 from the Department of Science and Technology, Government of India.

[1] J. J. Molitoris and H. Stöcker, Phys. Lett. **162B**, 47 (1985); G. F. Bertsch, W. G. Lynch, and M. B. Tsang, Phys. Lett. B **189**, 384 (1987).
[2] C. A. Ogilvie *et al.*, Phys. Rev. C **42**, R10 (1990).
[3] D. Krofcheck *et al.*, Phys. Rev. C **46**, 1416 (1992).
[4] D. J. Magestro, W. Bauer, O. Bjarki, J. D. Crispin, M. L. Miller, M. B. Tonjes, A. M. Vander Molen, G. D. Westfall, R. Pak, and E. Norbeck, Phys. Rev. C **61**, 021602(R) (2000).
[5] D. J. Magestro, W. Bauer, and G. D. Westfall, Phys. Rev. C **62**, 041603(R) (2000).
[6] D. Cussol *et al.*, Phys. Rev. C **65**, 044604 (2002).
[7] G. D. Westfall *et al.*, Phys. Rev. Lett. **71**, 1986 (1993).

[8] J. P. Sullivan *et al.*, Phys. Lett. B **249**, 8 (1990).
[9] J. C. Angelique *et al.*, Nucl. Phys. **A614**, 261 (1997).
[10] D. Krofcheck *et al.*, Phys. Rev. C **43**, 350 (1991).
[11] Z. Y. He *et al.*, Nucl. Phys. **A598**, 248 (1996).
[12] A. Buta *et al.*, Nucl. Phys. **A584**, 397 (1995).
[13] R. Pak *et al.*, Phys. Rev. Lett. **78**, 1022 (1997); R. Pak, O. Bjarki, S. A. Hannuschke, R. A. Lacey, J. Lauret, W. J. Llope, A. Nadasen, N. T. B. Stone, A. M. Vander Molen, and G. D. Westfall, Phys. Rev. C **54**, 2457 (1996); **53**, R1469 (1996).
[14] W. M. Zhang *et al.*, Phys. Rev. C **42**, R491 (1990); M. D. Partlan *et al.*, Phys. Rev. Lett. **75**, 2100 (1995); P. Crochet *et al.*, Nucl. Phys. **A624**, 755 (1997).
[15] B. A. Li, Phys. Rev. C **48**, 2415 (1993).
[16] V. de la Mota, F. Sebille, M. Farine, B. Remaud, and P. Schuck, Phys. Rev. C **46**, 677 (1992).
[17] H. M. Xu, Phys. Rev. C **46**, R389 (1992); Phys. Rev. Lett. **67**, 2769 (1991).
[18] H. Zhou, Z. Li, Y. Zhuo, and G. Mao, Nucl. Phys. **A580**, 627 (1994).
[19] E. Lehmann, A. Faessler, J. Zipprich, R. K. Puri, and S. W. Huang, Z. Phys. A **355**, 55 (1996).
[20] S. Soff, S. A. Bass, C. Hartnack, H. Stöcker, and W. Greiner, Phys. Rev. C **51**, 3320 (1995).
[21] S. Kumar, M. K. Sharma, R. K. Puri, K. P. Singh, and I. M. Govil, Phys. Rev. C **58**, 3494 (1998); S. Kumar, Ph.D. thesis, Panjab University, Chandigarh, 1999.
[22] A. D. Sood and R. K. Puri, Phys. Lett. B **594**, 260 (2004).
[23] A. D. Sood and R. K. Puri, Phys. Rev. C **69**, 054612 (2004)
[24] A. Sood and R. K. Puri, Symposium on Nuclear Physics (2002), Vol. 45B, p.288; A. Sood and R. K. Puri, in Proceedings of the VIII International Conference on Nucleus-Nucleus Collisions, Moscow, Russia, 2003.
[25] J. Aichelin, Phys. Rep. **202**, 233 (1991).
[26] C. Hartnack, R. K. Puri, J. Aichelin, J. Konopka, S. A. Bass, H. Stöcker, and W. Greiner, Eur. Phys. J. A **1**, 151 (1998).
[27] G. Peilert, H. Stöcker, W. Greiner, A. Rosenhauer, A. Bohnet, and J. Aichelin, Phys. Rev. C **39**, 1402 (1989); S. Kumar, R. K. Puri, and J. Aichelin, *ibid.* **58**, 1618 (1998); S. Kumar and R. K. Puri, *ibid.* **58**, 2858 (1998).
[28] J. Singh, S. Kumar, and R. K. Puri, Phys. Rev. C **62**, 044617 (2000); J. Singh and R. K. Puri, *ibid.* **62**, 054602 (2000).
[29] D. T. Khoa, N. Ohtsuka, A. Faessler, M. A. Matin, S. W. Huang, E. Lehmann, and Y. Lotfy, Nucl. Phys. **A542**, 671 (1992).
[30] W. Reisdorf, Nucl. Phys. **A630**, 15c (1998).
[31] B. Blättel, V. Koch, A. Lang, K. Weber, W. Cassing, and U. Mosel, Phys. Rev. C **43**, 2728 (1991).
[32] D. T. Khoa, N. Ohtsuka, M. A. Matin, A. Faessler, S. W. Huang, E. Lehmann, and R. K. Puri, Nucl. Phys. **A548**, 102 (1992); R. K. Puri, N. Ohtsuka, E. Lehmann, A. Faessler, M. A. Matin, D. T. Khoa, G. Batko, and S. W. Huang, *ibid.* **A575**, 733 (1994).
[33] G. F. Bertsch and S. Das Gupta, Phys. Rep. **160**, 189 (1988).
[34] D. Hahn and H. Stöcker, Nucl. Phys. **A452**, 723 (1986).
[35] L. Neise, M. Berenguer, C. Hartnack, G. Peilert, H. Stöcker, and W. Greiner, Nucl. Phys. **A519**, 375c (1990).
[36] A. Lang, B. Blättel, V. Koch, K. Weber, W. Cassing, and U. Mosel, Phys. Lett. B **245**, 147 (1990); A. Lang, B. Blättel, W. Cassing, V. Koch, U. Mosel, and K. Weber, Z. Phys. A **340**, 287 (1991).
[37] R. K. Puri, E. Lehmann, A. Faessler, and S. W. Huang, J. Phys. G **20**, 1817 (1994).
[38] R. K. Puri, E. Lehmann, N. Ohtsuka, A. Faessler, and S. W. Huang, in *Proceedings of the International Workshop XXII on Gross Properties of Nuclei and Nuclear Excitations*, Hirschegg, Austria, 1994, edited by H. Feldmeier and W. Noerenberg (GSI, Darmstadt, Germany), p. 262.